Journal of Molecular and Cellular Cardiology 85 (2015) 199–206

Contents lists available at ScienceDirect

Journal of Molecular and Cellular Cardiology

journal homepage: www.elsevier.com/locate/yjmcc

Original article

Phosphorylation of myosin regulatory light chain controls myosin head conformation in cardiac muscle

Thomas Kampourakis *, Malcolm Irving

Randall Division of Cell and Molecular Biophysics and British Heart Foundation Centre of Research Excellence, King's College London, London SE1 1UL, United Kingdom

ARTICLE INFO

Article history:
Received 11 April 2015
Received in revised form 18 May 2015
Accepted 3 June 2015
Available online 7 June 2015

Keywords:
Myosin
Cardiac muscle regulation
Myosin regulatory light chain
Polarized fluorescence
Regulatory light chain phosphorylation

ABSTRACT

The effect of phosphorylation on the conformation of the regulatory light chain (cRLC) region of myosin in ventricular trabeculae from rat heart was determined by polarized fluorescence from thiophosphorylated cRLCs labelled with bifunctional sulforhodamine (BSR). Less than 5% of cRLCs were endogenously phosphorylated in this preparation, and similarly low values of basal cRLC phosphorylation were measured in fresh intact ventricle from both rat and mouse hearts. BSR-labelled cRLCs were thiophosphorylated by a recombinant fragment of human cardiac myosin light chain kinase, which was shown to phosphorylate cRLCs specifically at serine 15 in a calcium- and calmodulin-dependent manner, both *in vitro* and *in situ*. The BSR-cRLCs were exchanged into demembranated trabeculae, and polarized fluorescence intensities measured for each BSR-cRLC in relaxation, active isometric contraction and rigor were combined with RLC crystal structures to calculate the orientation distribution of the C-lobe of the cRLC in each state. Only two of the four C-lobe orientation populations seen during relaxation and active isometric contraction in the unphosphorylated state were present after cRLC phosphorylation. Thus cRLC phosphorylation alters the equilibrium between defined conformations of the cRLC regions of the myosin heads, rather than simply disordering the heads as assumed previously. cRLC phosphorylation also changes the orientation of the cRLC C-lobe in rigor conditions, showing that the orientation of this part of the myosin head is determined by its interaction with the thick filament even when the head is strongly bound to actin. These results suggest that cRLC phosphorylation controls the contractility of the heart by modulating the interaction of the cRLC region of the myosin heads with the thick filament backbone.

1. Introduction

Contraction of both heart and skeletal muscle is driven by cyclic interactions between myosin and actin [1,2]. In each cycle, the light-chain domain (LCD) of the myosin head amplifies small conformational changes induced by the release of ATP hydrolysis products from its catalytic domain to produce large rotational motions of the LCD. One function of the LCD is thus to act as a 'lever arm' to generate nm-scale sliding between the myosin-containing thick filaments and the actin-containing thin filaments [3,4]. The part of the LCD next to the myosin head-rod junction is formed by the cardiac regulatory light chain (cRLC) winding around a short α-helix of the myosin heavy chain [5] (Fig. 1). The cRLC is thought to be partly phosphorylated *in vivo* under resting conditions, and some studies suggest that its phosphorylation level depends on the physiological state of the myocardium, implying a role for cRLC phosphorylation in the regulation of cardiac contractility [6–9]. Reported values of basal cRLC phosphorylation differ substantially however [10–12], and their interpretation is complicated by heterogeneity between different parts of the myocardium [7,13,14]. At a functional level, a significant role for cRLC phosphorylation is indicated by the effects of hypertrophic cardiomyopathy (HCM) mutations that abolish cRLC phosphorylation *in vitro* [15], and the severe cardiac dysfunction in transgenic mouse models expressing non-phosphorylatable cRLCs [12,16]. cRLC is phosphorylated by a cardiac-specific isoform of myosin light chain kinase (cMLCK) [17,18], and ablation of cMLCK expression is associated with a decrease in cRLC phosphorylation level in transgenic mice under basal conditions, leading to an impaired beta-adrenergic response and ventricular hypertrophy [19]. cMLCK activity has also been associated with control of sarcomere organisation in isolated mammalian cardiomyocytes [20] and with cardiac development in a zebrafish model [17]. However, the molecular mechanisms of these effects remain elusive.

The effects of cRLC phosphorylation on the mechanical properties of the myocardium have been extensively studied. Increased cRLC phosphorylation has been associated with an increase in calcium sensitivity [21], and in the rate of stretch activation [22] and cross-bridge cycling [23] in demembranated cardiac muscle preparations. The changes in

Abbreviations: cRLC, cardiac regulatory light chain; BSR, bifunctional sulforhodamine; cMyBP-C, cardiac myosin binding protein C; cMLCK, cardiac myosin light chain kinase; HMM, heavy meromyosin; ELC, essential light chain; LCD, light chain domain of myosin; ME, maximum entropy.

* Corresponding author.
E-mail address: thomas.kampourakis@kcl.ac.uk (T. Kampourakis).

http://dx.doi.org/10.1016/j.yjmcc.2015.06.002

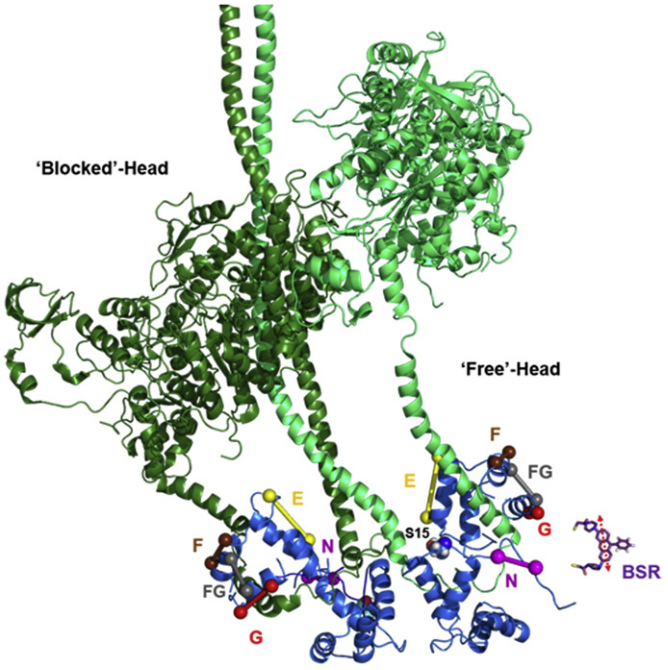

Fig. 1. Bifunctional rhodamine probes on the cRLC. The regulatory light chains (blue) are shown bound to the myosin heavy chain (green) in the atomic model for those regions of myosin in isolated thick filaments from invertebrate muscle (PDB 3DTP). The so-called 'blocked' and 'free' heads are shown in dark and light green, respectively. The essential light chains were removed for clarity. The model was built by superimposing the RLC structure of the nucleotide-free scallop myosin S1 (PDB 1SR6) onto the RLC of the free head, and by superimposing the RLC N- and C-lobes separately for the blocked head. The N-terminal extension of the RLC was built in Pymol using the sequence of human ventricular RLC. The phosphorylatable serine 15 is shown in Van der Waals representation. BSR probes were introduced on the RLC N-terminus (magenta), and helices E (yellow), F (brown), and G (red) and crosslinking helices F and G (grey) in the C-terminal lobe. The Cβ-atoms (or Cα-atoms in case of glycine residues) of mutated residues are shown as coloured spheres and the expected probe dipole orientations are indicated by sticks. The atomic structure of BSR (purple) is shown to scale in the right lower corner with the orientation of the fluorescence dipole indicated by a red double arrow.

the equatorial X-ray reflections from cardiac trabeculae produced by *in situ* cRLC phosphorylation indicate a transfer of myosin heads towards the thin filaments [23], suggesting that these mechanical effects may be mediated by an increased probability of actin attachment (for review see [11]). Electron microscopy studies of isolated thick filaments from mammalian and invertebrate skeletal muscles [24,25] showed that the helically ordered organisation of myosin heads on the thick filament surface in the unphosphorylated state is lost on incubation with active MLCK. However the molecular mechanism by which cRLC phosphorylation controls the conformation of the myosin heads is unknown.

We recently described a new method to determine the orientation of the cRLC region of the myosin heads with respect to the filament axis in demembranated ventricular trabeculae, based on measuring polarized fluorescence intensities from bifunctional sulforhodamine (BSR) probes on the cRLC [26]. We showed that, in the unphosphorylated state, cRLC orientation did not change significantly during calcium activation, and that its N-lobe did not change orientation even during strong attachment of myosin heads to actin in rigor. These results suggested that the cRLC interacts with the thick filament backbone *via* its N-lobe. Since the N-lobe contains the phosphorylation site, modulation of this interaction by cRLC phosphorylation might provide a mechanism for the control of myosin head conformation. Here we tested that hypothesis using a recombinant C-terminal fragment of the human cardiac isoform of MLCK to thiophosphorylate BSR-labelled human cRLCs *in vitro*. The BSR-cRLCs were exchanged into demembranated right ventricular trabeculae with a very low endogenous cRLC phosphorylation background, and the orientation of the phosphorylated cRLC C-lobe was determined during relaxation, active isometric contraction and rigor. An important advantage of this *in vitro* labelling/cRLC exchange approach is that the orientation of the phosphorylated cRLCs can be determined directly in the presence of a mixed phosphorylated/unphosphorylated population, since only the phosphorylated cRLCs carry the probe. Comparison with our previous results for unphosphorylated BSR-cRLCs using the same cRLC exchange protocol [26] then allowed us to determine the change in the *in situ* orientation of the C-lobe produced by cRLC phosphorylation in each state.

2. Materials and methods

Details of protein production, preparation of cardiac trabeculae, protein exchange protocols, fluorescence polarization experiments and tissue sampling procedures are provided in the supplemental materials.

3. Results

3.1. Preparative thiophosphorylation of BSR-cRLCs by cMLCK

A fragment of the human cardiac isoform of myosin light chain kinase (cMLCK, UniProtKB entry: Q32MK0) spanning the catalytic and regulatory domains was expressed in and purified from Sf9 cells to over 95% homogeneity as described in the Materials and methods section. The purified cMLCK fragment was partially phosphorylated (34% unphosphorylated, 55% mono- and 11% bis-phosphorylated as determined by Phostag™-SDS-PAGE; data not shown) and the phosphate groups were removed by Lambda Protein phosphatase treatment. There was no significant difference between the catalytic activities of the untreated and dephosphorylated cMLCK fragments.

Previous studies have led to contradictory conclusions about the calcium- and calmodulin-dependence of cMLCK activity [17,18]. In the present work, *in vitro* kinase assays at different enzyme-to-substrate ratios in the presence and absence of Ca^{2+}, calmodulin and EGTA revealed a strong dependence of cMLCK activity on Ca^{2+} and calmodulin (Fig. 2A), as expected from the canonical C-terminal calmodulin binding site of cMLCK. However, some calcium-independent catalytic activity was observed at high enzyme-to-substrate ratios.

Multiple phospho-species of cRLC have been identified in rodent cardiac muscle [27], and human cRLC contains several residues that could serve as potential substrates for protein kinases. Two serines in the N-terminal extension (S15 and S19) of cRLC and a tyrosine (Y118) in its C-lobe have been identified by mass spectrometry and site-specific methods as potentially phosphorylated *in vivo* (PhosphoSitePlus®, www.phosphosite.org) [28]. To unambiguously identify which residue is phosphorylated by the purified cMLCK (and to exclude the possible contribution of any co-purified kinases) we mutated the two serine residues (S15 and S19) in the N-terminal extension separately or together to alanines. The human wildtype and mutant cRLCs were tested in *in vitro* kinase assays (Fig. 2). Only the wildtype and S19A mutant could be phosphorylated, indicating that the purified cMLCK specifically phosphorylates serine 15 in the human cRLC N-terminal extension (Fig. 2A). Specific mono-phosphorylation of the recombinant wildtype cRLC was confirmed by ESI mass spectrometry. The measured (calculated) masses (in Da) for the cRLC before and after phosphorylation by cMLCK were 19020.6 (19020.5) and 19101.6 (19100.5), respectively. Additionally, although rat cRLC has an additional phosphorylatable serine at position 14 that is replaced by asparagine in the human cRLC sequence, we found that the recombinant cMLCK also mono-phosphorylates rat cRLC *in vitro* (Fig. S1), indicating that cMLCK has a high specificity for serine 15.

ATPγS was used to preparatively thiophosphorylate BSR-labelled cRLCs, on the basis that thiophosphorylated proteins are expected to be relatively resistant to dephosphorylation by any protein phosphatases that might be present in freshly skinned trabeculae. In this study,

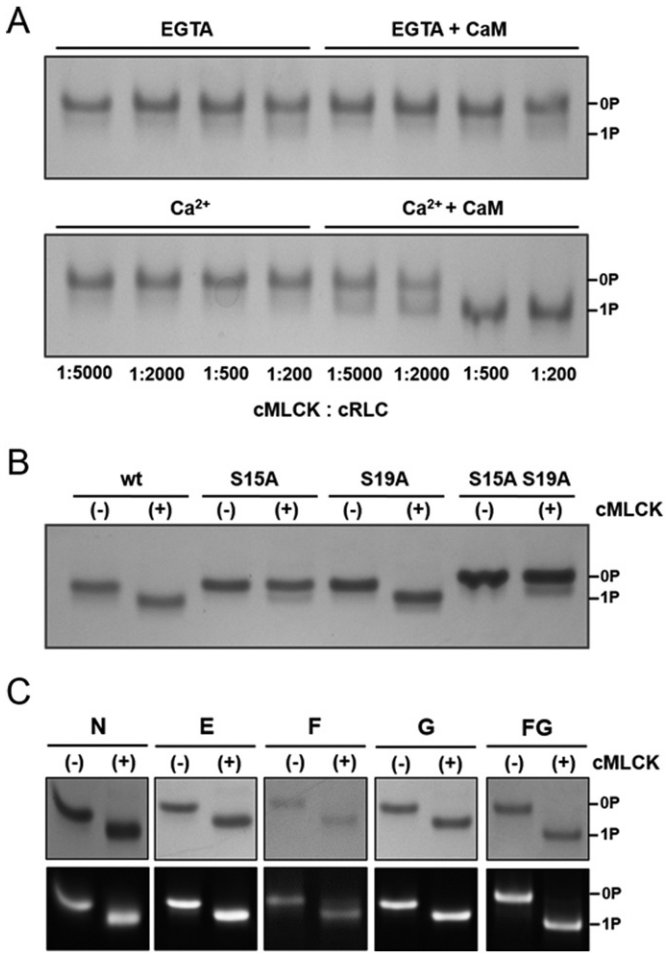

Fig. 2. Human cardiac myosin light chain kinase (cMLCK) phosphorylates the human ventricular cRLC at serine 15 in a calcium/calmodulin dependent manner. (A) Kinase assays at different cRLC to cMLCK stoichiometries in the absence or in the presence of calcium and calmodulin analysed by urea-glycerol PAGE. Note that the cRLC is significantly phosphorylated only in the presence of calcium and calmodulin. (B) Serine to alanine mutagenesis shows that cMLCK specifically phosphorylates serine 15 in the cRLC N-terminal extension ((−), control without cMLCK; (+), with cMLCK). (C) Bifunctional sulforhodamine labelled cRLC mutants were preparatively thiophosphorylated by cMLCK and the phosphorylation reaction analysed by urea-glycerol PAGE. Bands were visualized by Coomassie (top row) or by UV illumination (bottom row).

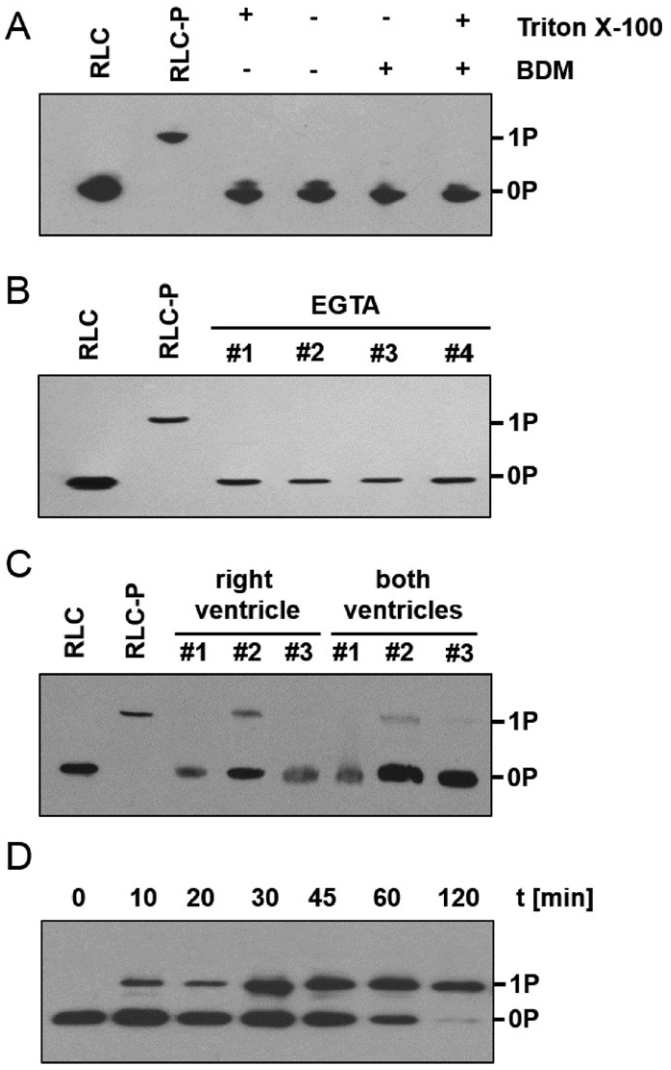

Fig. 3. Phosphorylation level of native cRLC in rat ventricle. (A) The effect of demembranation with Triton X-100 and BDM treatment on the cRLC phosphorylation level of right ventricular trabeculae was assessed by Phostag™-SDS-PAGE and subsequent Western-Blot against cRLC. No significant cRLC phosphorylation was observed independent of the treatment (standards: RLC, recombinant RLC; RLC-P, recombinant RLC mono-phosphorylated with cMLCK). (B) Replacement of 2.5 mM Ca^{2+} with 1 mM EGTA in the cardioplegia solution used to prepare trabeculae had no significant effect on the RLC phosphorylation level. (C) Lysate of whole right ventricular tissue and mixture of right and left ventricular tissue was probed for cRLC phosphorylation level. The phosphorylation levels were estimated by densitometric analysis in ImageJ to be 0.05 ± 0.03 mol P_i/mol RLC and 0.03 ± 0.02 mol P_i/mol RLC (mean ± SEM, n = 3) for the right ventricle and both ventricles, respectively. (D) *In-situ* phosphorylation of cRLC. Skinned trabecular preparations were incubated with cMLCK, samples were taken at the indicated time points and the extent of RLC phosphorylation measured by Phostag™ SDS-PAGE and Western blot.

only thiophosphorylated cRLCs labelled on the C-terminal lobe were used (Fig. 1), because labelling of helices in the N-terminal lobe (particularly the A- and D-helices) interfered with phosphorylation of the cRLCs by cMLCK (Fig. S2). Surprisingly, BSR-crosslinking of cysteine residues introduced at positions 6 and 10, relatively close to the phosphorylatable serine residue 15, did not significantly interfere with the phosphorylation reaction (Fig. 2C). All cRLCs with probes attached in the C-terminal lobe (BSR-cRLCs E, F, G and FG) were preparatively mono-thiophosphorylated within 2 h to 4 h to over 95% homogeneity (Fig. 2C).

3.2. Native cRLC phosphorylation level

The distribution of phosphorylated cRLC species in rat trabeculae was measured by Phostag™-SDS-PAGE [29] followed by Western Blot against cRLC (Fig. 3). The endogenous cRLCs in demembranated trabeculae were almost entirely dephosphorylated. Neither the skinning procedure nor treatment of the tissue with 2,3-butanedione monoxime (BDM) or calcium had a significant effect on the cRLC phosphorylation level (Figs. 3A and 3B), suggesting that the low cRLC phosphorylation level might be endogenous to rat trabeculae under basal conditions. Tissue samples removed and snap-frozen immediately (within two minutes) after sacrificing the animal also showed a homogenously low cRLC phosphorylation level in the right and left ventricles (Fig. 3C), further supporting this conclusion. Incubation of skinned trabeculae with 1 μM cMLCK led to almost full phosphorylation of the endogenous cRLCs within 2 h (Fig. 3D). The recombinant cMLCK only mono-phosphorylated the endogenous cRLCs *in situ*, consistent with the *in vitro* phosphorylation data described above (Fig. S1).

A similarly low endogenous cRLC phosphorylation level was observed for mouse ventricular tissue (Fig. S3). Freshly prepared whole ventricular samples and the enriched myofibrillar fraction showed a homogenously low cRLC phosphorylation level, indicating

that sample preparation did not affect the cRLC phosphorylation level measurements.

3.3. Exchange of thiophosphorylated BSR-cRLCs into skinned trabeculae

Thiophosphorylated BSR-cRLCs (subsequently referred to as 'phosphorylated') were exchanged into skinned trabeculae from rat right ventricle by bathing the trabeculae in EDTA rigor solution containing 0.5 mg/ml of the phosphorylated BSR-cRLC for 30 min at 22 °C. Subsequently, the trabeculae were bathed in relaxing solution containing 0.5 mg/ml cTnC and cTn for 20 min and 1 h, respectively to replace any of these proteins lost during cRLC exchange. The extent of exchange was estimated by SDS-PAGE followed by either Coomassie staining or by Western Blot against cRLC (Fig. S4), which allowed separation of the endogenous and phosphorylated BSR-labelled cRLCs. Densitometric analysis of the Coomassie-stained gels showed that about 30% of the endogenous cRLCs were replaced by phosphorylated BSR-cRLC-G. In contrast, SDS-PAGE followed by Western Blot against cRLC indicated that 18% ± 2% of the endogenous cRLCs were replaced. Similar exchange ratios were obtained for the other phosphorylated BSR-cRLCs (12% ± 6%, 20% ± 5% and 14% ± 8% for BSR-cRLC-E, -F and -FG, respectively, mean ± SD; n = 3), in approximate agreement with the exchange fraction of 12% for the unphosphorylated BSR-cRLCs estimated by fluorescence intensity [26]. Incorporation of phosphorylated BSR-cRLCs had no effect on the protein stoichiometry of skinned ventricular trabeculae (Fig. S5), but the phosphorylation levels of cTnI and cMyBP-C decreased. In the case of cTnI this effect may be due to replacement of endogenous phosphorylated troponin lost during the cRLC exchange protocol with recombinant unphosphorylated troponin complex (see Materials and Methods). The origin of the lower cMyBP-C phosphorylation observed following the cRLC exchange protocol is unknown.

Replacement of 10%–30% of the endogenous unphosphorylated cRLC with phosphorylated BSR-cRLC had no significant effect on maximal force at pCa 4.5 and 2.1 μm sarcomere length; force recovery after cRLC exchange of un- and phosphorylated BSR-cRLCs was 88% ± 11% (mean ± SD; n = 25) and 88% ± 9% (mean ± SD; n = 23), respectively.

3.4. Polarized fluorescence from phosphorylated BSR-cRLCs

The polarized fluorescence intensities obtained from the BSR probes on the N-terminus, on the E, F, G helices and crosslinking the F and G helices (subsequently referred to as FG) of the phosphorylated cRLCs (Fig. 1) were used to calculate the order parameters $\langle P_{2d} \rangle$, which describes the amplitude of the independent motion ("wobble") of the probe on the surface of the cRLC on the sub-nanosecond timescale, and $\langle P_2 \rangle$ and $\langle P_4 \rangle$, which describe the time-averaged orientation of the probe fluorescence dipoles with respect to the filament axis [30]. $\langle P_{2d} \rangle$ can take values between 0 and 1, these extreme values indicating isotropic motion on the fluorescence timescale or total immobilization of the probe on the surface of the protein, respectively. Since BSR labelled cRLCs were mono-phosphorylated to homogeneity *in vitro*, measured order parameters are exclusively from myosin heads carrying the phosphorylated BSR-cRLCs.

$\langle P_{2d} \rangle$ for all probes except FG changed significantly upon phosphorylation (Fig. S6). $\langle P_{2d} \rangle$ for the N-, E- and G-helix probes increased from about 0.6 to about 0.75, indicating less mobility of these probes on the sub-nanosecond timescale. In contrast, $\langle P_{2d} \rangle$ for the F-helix probe decreased on phosphorylation, from around 0.9 to 0.75. These changes in $\langle P_{2d} \rangle$ on phosphorylation are much larger than those associated with calcium activation or binding of myosin heads to actin in rigor. The latter interventions did not produce significant changes in $\langle P_{2d} \rangle$ for probes on either the C- or N-lobe of cRLC [26], and similar results were reported previously for probes on the N- and C-lobes of the RLC in skeletal muscle [31,32]. The large changes in $\langle P_{2d} \rangle$ for the N, E, F and G helix probes on phosphorylation suggest that the local environment of these probes has been substantially altered. This might be due to an intermolecular interaction between the probe and another thick filament component, or between the N-terminal extension and the C-lobe of the cRLC (see Discussion).

To describe the time-averaged orientation of the probes in a more physically meaningful manner, we calculated the peak angle θ_{ME} and standard deviation σ_{ME} of the probe orientation distributions with respect to the trabecular axis from the measured order parameters $\langle P_2 \rangle$ and $\langle P_4 \rangle$ using a maximum entropy formalism (Fig. S6). The BSR probe attached to the cRLC N-terminal extension (BSR-cRLC-N) showed the same peak angle under all experimental conditions, independent of phosphorylation. For BSR-cRLC-E and -F, phosphorylation increased the peak angle θ_{ME} during relaxation towards the value measured during active isometric contraction in the dephosphorylated state, but did not change θ_{ME} significantly during active isometric contraction and rigor. σ_{ME} decreased for BSR-cRLC-E in relaxation and active contraction, but increased for BSR-cRLC-F in all three states. The largest changes in the angular distribution were observed for BSR-cRLC-G, with an increase in θ_{ME} under all experimental conditions. Phosphorylation did not significantly change the angular distribution of BSR probes crosslinking helices F and G. The implications of these changes are best understood by combining the results from the different probes to calculate the overall orientation of the cRLC C-lobe in each state, as described below.

3.5. Orientation of the phosphorylated cRLC C-lobe in ventricular trabeculae

The orientation of the cRLC C-lobe was described in terms of its local EG-helix frame (see Materials and Methods section), with β describing the angle between the E-helix and the filament axis, and γ describing rotation of the C-lobe around the E-helix. We showed previously that the orientation distribution of the unphosphorylated cRLC C-lobe in relaxation and active contraction (Fig. 4A) can be described in terms of four populations, referred to as C1 to C4 in order of increasing β [26]. There is very little change in the unphosphorylated cRLC C-lobe orientation distribution on calcium activation, but the C1 and C3 peaks become much weaker in rigor. An analogous study of the unphosphorylated cRLC N-lobe showed similar orientation distributions in relaxation, active isometric contraction and rigor [26], suggesting that the cRLC region of myosin might stays docked onto the thick filament backbone through interactions with the cRLC N-lobe in all these states when the cRLC is unphosphorylated.

When the cRLC is phosphorylated (Fig. 4B), the orientation distributions of the C-lobe of the cRLC in relaxation and isometric contraction show two main peaks, corresponding to the C2 and C3 peaks seen for the unphosphorylated cRLC, with $(\beta_{EG}, \gamma_{EG}) = (60°, -60°)$ and (85°, 35°), respectively. Phosphorylated cRLC C-lobes are less likely to be in the more parallel orientations C1 and C4, with $(\beta_{EG}, \gamma_{EG}) = (30°, 15°)$ and (125°, −30°), respectively. Qualitatively similar effects of phosphorylation on cRLC C-lobe orientation were observed when different cRLC reference structures were used for the ME calculations (Fig. S7). Thus the conclusions about the effects of cRLC phosphorylation on its orientation are unlikely to be influenced by a change in the overall fold of the light chain domain, which is almost unaffected by phosphorylation *in vitro* [33]. The orientation distributions in Fig. 4 were also not significantly affected by the experimental variability in the order parameters $\langle P_2 \rangle$ and $\langle P_4 \rangle$ (Tab. S1), as shown by repeating the ME calculations with values chosen at random from normal distributions of the measured order parameters (Fig. S8).

As noted previously [26], peak C4 of the cRLC C-lobe orientation distribution, which is more prominent in the unphosphorylated state (Fig. 4A), is close to the orientations of the RLC C-lobe in the myosin heads in isolated thick filaments from invertebrate skeletal muscle (Fig. 1) [34]. In this asymmetric structure, sometimes called the 'J-motif' or 'interacting heads motif', which seems to be conserved among muscle types and species [35,36], the myosin heads are folded

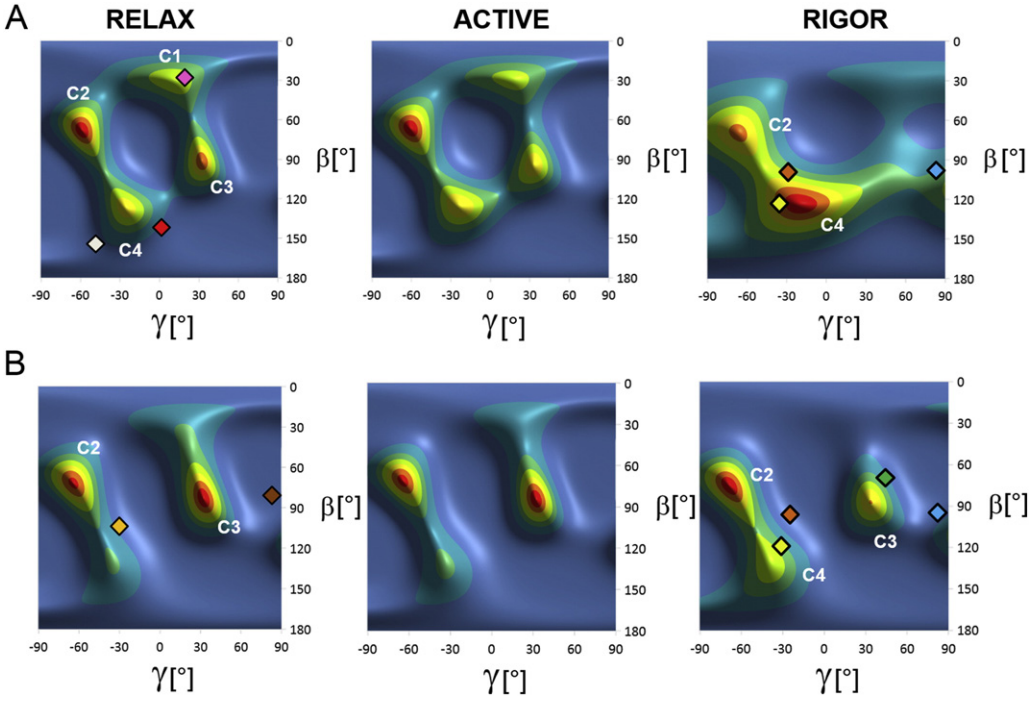

Fig. 4. Orientation distributions of the cRLC C-lobe in ventricular trabeculae during relaxation (RELAX), active isometric contraction (ACTIVE) and rigor calculated from the order parameters measured from unphosphorylated (A) and phosphorylated BSR-cRLCs (B), using the structure of scallop myosin S1 in the nucleotide-free state (PDB entry 1SR6). The calculated cRLC C-lobe orientations (β,γ) for the blocked and free heads (PDB entry 3DTP), and 'phos-free-like' and 'phos-blocked-like' (PDB entry 3J04) aligned by their S2 regions are indicated by red and white, and brown and light orange diamonds, respectively. The calculated orientations for nucleotide-free chicken skeletal S1 (PDB entry 2MYS) and scallop S1 (PDB entry 1SR6), ADP-bound squid S1 (PDB entry 3I5F), pre-power-stroke scallop S1 (PDB entry 1QVI), and smooth muscle S1 in the ADP.Pi state (1BR1), with their catalytic domains superimposed onto the nucleotide-free chicken skeletal myosin S1 in the actin-S1 rigor complex, are shown as orange, yellow, cyan, green and pink diamonds respectively.

back against the filament backbone. The calculated orientations of the 'blocked' and 'free' heads of the J-motif are indicated by red and white diamonds in Fig. 4A. The weakening of the C4 peak on cRLC phosphorylation (Fig. 4B) therefore suggests that the J-motif is disrupted by cRLC phosphorylation. The more perpendicular C2 and C3 orientations that dominate the orientation maps for phosphorylated cRLC are more similar to those observed in 2D crystals of isolated phosphorylated HMM from smooth muscle [37] (PDB entry 3J04). These are shown as the brown and orange diamonds in Fig. 4B, for the so-called phospho-free-like and phospho-blocked-like heads respectively. Although these orientations are roughly perpendicular to the filament axis, like the C2 and C3 peaks, they have a different twist angle γ.

The orientation of the C-lobe of phosphorylated cRLC did not change significantly during the transition from relaxation to active isometric contraction (Fig. 4B). Thus the C-lobe orientation is almost insensitive to calcium activation, as reported previously for the unphosphorylated cRLC (Fig. 4A) [26]. Peaks C2 and C3 for phosphorylated cRLC remained strong in rigor (Fig. 4B), but C4 was stronger than in relaxation or active contraction. The rigor orientation distribution depends strongly on cRLC phosphorylation, with C4 much weaker but C3 much stronger in the phosphorylated state (compare Fig. 4B with Fig. 4A). Since all myosin heads are thought to be strongly bound to actin in rigor, these cRLC C-lobe orientations can be compared with those expected when the catalytic domains of published myosin head or S1 structures are docked onto that of the canonical actin-S1 rigor complex [38]. The resulting C-lobe orientations for nucleotide-free S1s from chicken and scallop muscle, shown as the orange and yellow diamonds in Fig. 4 (Rigor), are close but not identical to peak C4. Squid S1 with bound ADP (cyan) is close to the symmetry-related equivalent of C2, scallop muscle S1 in the pre-power-stroke state (green) is close to C3, and chicken smooth muscle S1 in the pre-power-stroke state (pink) is close to C1 respectively. These comparisons emphasize the diversity of relative orientations of the light-chain and catalytic domains in published S1 crystal structures, a diversity that is matched by that of the cRLC C-lobe orientations in cardiac muscle cells.

4. Discussion

4.1. Phosphorylation level of endogenous ventricular myosin regulatory light chain

As noted in the Introduction, there is no clear consensus about the basal level of cRLC phosphorylation in mammalian cardiac muscle. Some studies have reported a constant level of 0.4–0.5 mol P_i/mol cRLC [39] (for review see [11]), whereas others have reported much lower ventricular RLC phosphorylation levels [6,12,40]. These differences may be associated with heterogeneity between different parts of the heart [7,13,41] and potential effects of species, gender and tissue sampling procedures [42].

The cardiac muscle preparations from rat ventricle used in the present experiments had a consistently low cRLC phosphorylation level of less than 0.05 mol P_i/mol cRLC, and this was independent of the tissue treatment. Moreover the same low level was measured in the intact ventricle immediately snap-frozen after excision (Fig. 3). Freshly prepared mouse heart myofibrils and whole ventricular preparations that were immediately snap-frozen after excision of the heart showed that the mouse cRLCs are also almost entirely unphosphorylated (Fig. S3) suggesting that the low ventricular cRLC phosphorylation level is conserved among rodent species and independent of the sample preparation. Similar low cRLC phosphorylation levels were recently measured in swine myocardium by mass spectrometry [10], suggesting that the basal phosphorylation level of mammalian cRLCs might be lower or more dynamic than previously thought.

An increase in cRLC phosphorylation level in intact cardiac muscle has been associated with an increase in the stimulation frequency,

muscle pre-load, and isoprenaline treatment [6–9], suggesting that these stimuli work upstream of cRLC phosphorylation and might be involved in the activation of cardiac myosin light chain kinase (cMLCK). Prolonged incubation of skinned cardiac muscle preparations with recombinant cMLCK led to almost full phosphorylation of the endogenous cRLCs in our preparations, suggesting that both cRLCs of the double-headed myosin molecule are available for phosphorylation by cMLCK *in situ*. However, the cMLCK phosphorylated the cRLCs to a maximum level of ca 1 mol/mol both *in situ* and *in vitro*, suggesting that different signalling pathways are involved in the *multiple* phosphorylated cRLC species identified in rodent cardiac muscle *in vivo* [43–45].

4.2. Effects of phosphorylation on cRLC dynamics

Phosphorylation of the cRLC produced significant changes in the order parameter $\langle P_{2d} \rangle$ for the BSR probes (Table S1), which describes the amplitude of fast probe motion ("wobble") on the surface of the cRLC. The observed changes were much larger than those associated with the transition from relaxation to active isometric contraction or rigor, suggesting that cRLC phosphorylation leads to a much larger change in the local environment of the probes. These effects were not confined to the probe close to the phosphorylatable serine 15 in the cRLC N-terminal extension (BSR-cRLC-N), suggesting that they are due to global changes in cRLC environment associated with changes in its tertiary structure or with intermolecular interactions. The observation that the crystal structure of the scallop smooth muscle light chain domain does not change significantly on RLC phosphorylation [33] argues against the former explanation.

A more likely explanation, suggested previously as a mechanism for activation of smooth muscle contraction by RLC phosphorylation [46], is that interactions between the cRLC N-terminal extension and other regions on the surface of the cRLC are altered by phosphorylation of serine 15. A similar mechanism was recently proposed for the effect of phosphorylation of serines 22/23 of cardiac troponin I, involving contacts between positively charged residues in its N-terminal extension, close to serines 22/23, and negatively charged residues in the N-lobe of troponin C [47].

4.3. cRLC phosphorylation controls myosin head orientation in diastole and systole

The distribution of the orientations of phosphorylated cRLC with respect to the thick filament axis in the relaxed (low calcium or diastolic) state showed two distinct peaks (Fig. 4B), in contrast with the four described previously for unphosphorylated cRLC (Fig 4A). The more parallel orientations C1 and C4 become much weaker on phosphorylation, and the more perpendicular orientations, C2 and C3, dominate the distributions in the phosphorylated state. The orientation distribution of the cRLC C-lobe is therefore *more* ordered in the phosphorylated state, in contrast with the overall distribution of myosin head conformations inferred from electron-microscopy studies on isolated thick filaments from invertebrate [25,48] and vertebrate muscle [24], which are disordered in the phosphorylated state. Thus, at the level of the cRLC region of myosin, phosphorylation shifts the conformational equilibrium towards perpendicular states rather than inducing disorder of this region, although the catalytic domains of the heads may be more orientationally disordered in the phosphorylated state.

The C4 orientation seen in the unphosphorylated state is similar to that in the free and blocked heads of the 'J motif' or 'interacting heads motif' conformation seen by EM of isolated filaments, in which the myosin heads are close to the thick filament backbone [34–36], in an 'OFF' or 'super-relaxed' state of the thick filament [49]. The C1 peak, being even more parallel to the filament axis, might also correspond to a folded state (Fig. 5). However it is also possible that the C1 peak, with an orientation similar to that expected for actin-bound myosin heads in the pre-powerstroke or transition state (pink diamond in Fig. 4A),

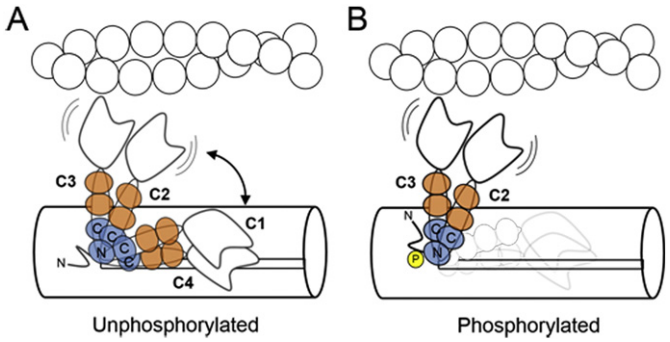

Fig. 5. Schematic model for the effect of cRLC phosphorylation on myosin head orientation. (A) Unphosphorylated myosin heads are in a conformational equilibrium between more parallel 'ON'-states (peaks C1 and C4, Fig. 4) and more perpendicular 'OFF'-states (peaks C2 and C3), controlled by the interaction of the cRLC with the thick filament surface. The cRLC and ELC are shown in blue and orange, respectively. The N- and C-terminal lobes of the cRLC are labelled accordingly. (B) Phosphorylation of cRLC destabilizes the parallel 'OFF'-conformations (C1 and C4) promoting attachment of the catalytic domain of myosin to actin.

corresponds to myosin heads that are weakly attached to actin in relaxing or diastolic conditions.

Phosphorylation of the cRLC weakens both the C1 and C4 peaks, reducing the number of myosin heads in the 'super relaxed' state or 'OFF' state of the thick filament (Fig. 5). The perpendicular C2 and C3 peaks become more prominent (Fig. 4B), and this perpendicular conformation would lead to the heads extending out from the thick filament backbone, bringing their motor domains closer to the thin filament and promoting interaction with actin (Fig. 5). Such a motion of myosin heads towards the thin filaments on phosphorylation is consistent with X-ray studies on skinned cardiac muscle [23], and with the increase in calcium sensitivity associated with cRLC phosphorylation [21]. A similar mechanism has been proposed for the functional effects of RLC phosphorylation in the indirect flight muscles of insects [50].

In contrast with the large effects of cRLC phosphorylation described above, the orientation of the cRLC region did not change significantly on calcium activation in either the phosphorylated or unphosphorylated states, suggesting that strong attachment of myosin to actin during active contraction (in systole) does not alter the orientation of the C-lobe of cRLC. This is consistent with our previous conclusion [26] that the primary function of the cRLC region of myosin is to regulate the availability of myosin heads for attachment to actin. The present results show that this transition between the 'OFF' and 'ON' conformations of the myosin heads is controlled by the phosphorylation state of the cRLC (Fig. 5).

One potential limitation of the present experiments is that less than 30% of endogenous unphosphorylated rat cRLCs were replaced by phosphorylated BSR-RLCs, so that the majority of myosin heads in the trabeculae were unphosphorylated. Although the *in vitro* phosphorylation and labelling protocol used here specifically measures the orientation of the phosphorylated cRLCs within a mixed population of phosphorylated and unphosphorylated myosin heads *in situ*, we cannot exclude the possibility that intra- or intermolecular interactions between the heads [35,36] might attenuate the observed effects of phosphorylation when a low fraction of heads are phosphorylated. Such an effect would imply that an even larger effect of cRLC phosphorylation on its orientation distribution might be observed at higher phosphorylation levels, and might explain the residual C1 and C4 features seen for the phosphorylated cRLCs in relaxation and active contraction in the present experiments (Fig. 4B). However, given the very low level of basal cRLC phosphorylation in the preparation used here, the levels of cRLC phosphorylation achieved here are likely to be in the physiological range. The present results clearly establish that relatively low changes in phosphorylation level in this range are sufficient to produce significant

changes in cRLC orientation, consistent with previous studies on isolated thick filaments from vertebrate skeletal muscle, in which phosphorylation of only 10% of the RLCs was sufficient to disorder the helical array of myosin heads [24].

4.4. Structural mechanism for the thick filament-based regulation of cardiac contractility by cRLC phosphorylation

Since the cRLC region of the myosin heads remains ordered after cRLC phosphorylation (Fig. 4B), even in the calcium-activated systolic state, the present results suggest that an interaction between the cRLC and the thick filament backbone is maintained after cRLC phosphorylation. Thus the present results imply a modification of the mechanism by which RLC phosphorylation controls the conformation of the myosin heads suggested previously by electron micrographs of isolated thick filaments from invertebrates [25,48] and vertebrates [24], and by X-ray diffraction studies on skinned mammalian cardiac muscle [23]. Those studies suggested that the effect of RLC phosphorylation on myosin head conformation was mediated by a weakening or breaking of the interaction between cRLC and the filament backbone; the present results, in contrast, suggest that the cRLC region of myosin stays bound to the thick filament backbone in a preferred conformation. The effect of RLC phosphorylation is to shift the conformational equilibrium between distinct RLC: backbone interactions that correspond to distinct RLC orientations and by implication distinct conformations of the myosin motor domain (Fig. 5).

The effect of cRLC phosphorylation on actin-bound myosin heads in rigor provides further support for the above conclusion. In the unphosphorylated state, the cRLC C-lobe adopts a conformation (Fig. 4; peak C4) similar to that of nucleotide-free scallop myosin S1 in the rigor complex (Fig. 4; yellow diamond). After phosphorylation, however, the predominant orientations are those populated during relaxation and active contraction (peaks C2 and C3), and C4 becomes a minor population. Since cRLC phosphorylation is unlikely to change the actin-interaction of the catalytic domain in rigor, this change in cRLC orientation implies a phosphorylation-mediated change in the preferred conformation of the cRLC on the thick filament surface in a myosin head that is strongly bound to actin. It follows that all or part of the cRLC is not part of the functional lever arm of the myosin motor in cardiac muscle, which would therefore be shorter than previously assumed [26]. This effect may require an intact thick filament, since cRLC phosphorylation leads to an increase in mean step-size in isolated cardiac myosin [51].

Control of myosin head conformation by mediating conformational states of cRLC at its interaction point with the thick filament might represent a common mechanism for thick filament-based control of cardiac contractility. The interactions of cRLC with the N-terminus of cMyBP-C [52] and with the A-band region of titin [36] could also feed into this regulatory pathway to constrain the conformational and regulatory state of the myosin heads.

5. Conclusions

We found that the basal *in vivo* cRLC phosphorylation level in the rodent heart is lower than previously thought, at less than 0.05 mol P_i/mol cRLC. Serine 15 of cRLC is phosphorylated by cMLCK in a calcium/calmodulin dependent manner. cRLC phosphorylation does not disorder the cRLC region of the myosin heads, but alters the conformational equilibrium towards states in which the heads can interact more readily with the thin filament. cRLC phosphorylation controls myosin head orientation and the contractility of the heart by modulating interactions between the cRLC region of myosin and the thick filament backbone.

Disclosures

None

Acknowledgments

We are grateful to the British Heart Foundation (PG/12/52/29713) for financial support and Dr. Martin Reese and Birgit Brandmeier for supplying the calmodulin used in this study. We further thank David Trentham, Mathias Gautel, Katherina Jenniches, Phillip Marshal and Yin-Biao Sun for help and advice.

Appendix A. Supplementary data

Supplementary data to this article can be found online at http://dx.doi.org/10.1016/j.yjmcc.2015.06.002.

References

[1] Huxley HE. The mechanism of muscular contraction. Science 1969;164:1356–65.
[2] Lymn RW, Taylor EW. Mechanism of adenosine triphosphate hydrolysis by actomyosin. Biochemistry 1971;10:4617–24.
[3] Irving M, St Claire Allen T, Sabido-David C, Craik JS, Brandmeier B, Kendrick-Jones J, et al. Tilting of the light-chain region of myosin during step length changes and active force generation in skeletal muscle. Nature 1995;375:688–91.
[4] Holmes KC. The swinging lever-arm hypothesis of muscle contraction. Curr Biol 1997;7:R112–8.
[5] Rayment I, Rypniewski WR, Schmidt-Base K, Smith R, Tomchick DR, Benning MM, et al. Three-dimensional structure of myosin subfragment-1: a molecular motor. Science 1993;261:50–8.
[6] Silver PJ, Buja LM, Stull JT. Frequency-dependent myosin light chain phosphorylation in isolated myocardium. J Mol Cell Cardiol 1986;18:31–7.
[7] Dias FA, Walker LA, Arteaga GM, Walker JS, Vijayan K, Pena JR, et al. The effect of myosin regulatory light chain phosphorylation on the frequency-dependent regulation of cardiac function. J Mol Cell Cardiol 2006;41:330–9.
[8] Verduyn SC, Zaremba R, van der Velden J, Stienen GJ. Effects of contractile protein phosphorylation on force development in permeabilized rat cardiac myocytes. Basic Res Cardiol 2007;102:476–87.
[9] Monasky MM, Biesiadecki BJ, Janssen PM. Increased phosphorylation of tropomyosin, troponin I, and myosin light chain-2 after stretch in rabbit ventricular myocardium under physiological conditions. J Mol Cell Cardiol 2010;48:1023–8.
[10] Peng Y, Gregorich ZR, Valeja SG, Zhang H, Cai W, Chen YC, et al. Top-down proteomics reveals concerted reductions in myofilament and Z-disc protein phosphorylation after acute myocardial infarction. Mol Cell Proteomics 2014;13:2752–64.
[11] Scruggs SB, Solaro RJ. The significance of regulatory light chain phosphorylation in cardiac physiology. Arch Biochem Biophys 2011;510:129–34.
[12] Sanbe A, Fewell JG, Gulick J, Osinska H, Lorenz J, Hall DG, et al. Abnormal cardiac structure and function in mice expressing nonphosphorylatable cardiac regulatory myosin light chain 2. J Biol Chem 1999;274:21085–94.
[13] Davis JS, Hassanzadeh S, Winitsky S, Lin H, Satorius C, Vemuri R, et al. The overall pattern of cardiac contraction depends on a spatial gradient of myosin regulatory light chain phosphorylation. Cell 2001;107:631–41.
[14] Sheikh F, Ouyang K, Campbell SG, Lyon RC, Chuang J, Fitzsimons D, et al. Mouse and computational models link Mlc2v dephosphorylation to altered myosin kinetics in early cardiac disease. J Clin Invest 2012;122:1209–21.
[15] Szczesna D, Ghosh D, Li Q, Gomes AV, Guzman G, Arana C, et al. Familial hypertrophic cardiomyopathy mutations in the regulatory light chains of myosin affect their structure, Ca2 + binding, and phosphorylation. J Biol Chem 2001;276:7086–92.
[16] Scruggs SB, Hinken AC, Thawornkaiwong A, Robbins J, Walker LA, de Tombe PP, et al. Ablation of ventricular myosin regulatory light chain phosphorylation in mice causes cardiac dysfunction *in situ* and affects neighboring myofilament protein phosphorylation. J Biol Chem 2009;284:5097–106.
[17] Seguchi O, Takashima S, Yamazaki S, Asakura M, Asano Y, Shintani Y, et al. A cardiac myosin light chain kinase regulates sarcomere assembly in the vertebrate heart. J Clin Invest 2007;117:2812–24.
[18] Chan JY, Takeda M, Briggs LE, Graham ML, Lu JT, Horikoshi N, et al. Identification of cardiac-specific myosin light chain kinase. Circ Res 2008;102:571–80.
[19] Ding P, Huang J, Battiprolu PK, Hill JA, Kamm KE, Stull JT. Cardiac myosin light chain kinase is necessary for myosin regulatory light chain phosphorylation and cardiac performance *in vivo*. J Biol Chem 2010;285:40819–29.
[20] Aoki H, Sadoshima J, Izumo S. Myosin light chain kinase mediates sarcomere organization during cardiac hypertrophy *in vitro*. Nat Med 2000;6:183–8.
[21] Olsson MC, Patel JR, Fitzsimons DP, Walker JW, Moss RL. Basal myosin light chain phosphorylation is a determinant of Ca2 + sensitivity of force and activation dependence of the kinetics of myocardial force development. Am J Physiol Heart Circ Physiol 2004;287:H2712–8.
[22] Stelzer JE, Patel JR, Moss RL. Acceleration of stretch activation in murine myocardium due to phosphorylation of myosin regulatory light chain. J Gen Physiol 2006;128:261–72.
[23] Colson BA, Locher MR, Bekyarova T, Patel JR, Fitzsimons DP, Irving TC, et al. Differential roles of regulatory light chain and myosin binding protein-C phosphorylations in the modulation of cardiac force development. J Physiol 2010;588:981–93.
[24] Levine RJ, Kensler RW, Yang Z, Stull JT, Sweeney HL. Myosin light chain phosphorylation affects the structure of rabbit skeletal muscle thick filaments. Biophys J 1996;71:898–907.

[25] Craig R, Padron R, Kendrick-Jones J. Structural changes accompanying phosphorylation of tarantula muscle myosin filaments. J Cell Biol 1987;105:1319–27.
[26] Kampourakis T, Sun YB, Irving M. Orientation of the N- and C-terminal lobes of the myosin regulatory light chain in cardiac muscle. Biophys J 2015;108:304–14.
[27] Scruggs SB, Reisdorph R, Armstrong ML, Warren CM, Reisdorph N, Solaro RJ, et al. A novel, in-solution separation of endogenous cardiac sarcomeric proteins and identification of distinct charged variants of regulatory light chain. Mol Cell Proteomics 2010;9:1804–18.
[28] Hornbeck PV, Kornhauser JM, Tkachev S, Zhang B, Skrzypek E, Murray B, et al. PhosphoSitePlus: a comprehensive resource for investigating the structure and function of experimentally determined post-translational modifications in man and mouse. Nucleic Acids Res 2012;40:D261–70.
[29] Kinoshita E, Kinoshita-Kikuta E, Takiyama K, Koike T. Phosphate-binding tag, a new tool to visualize phosphorylated proteins. Mol Cell Proteomics 2006;5:749–57.
[30] Dale RE, Hopkins SC, an der Heide UA, Marszalek T, Irving M, Goldman YE. Model-independent analysis of the orientation of fluorescent probes with restricted mobility in muscle fibers. Biophys J 1999;76:1606–18.
[31] Brack AS, Brandmeier BD, Ferguson RE, Criddle S, Dale RE, Irving M. Bifunctional rhodamine probes of myosin regulatory light chain orientation in relaxed skeletal muscle fibers. Biophys J 2004;86:2329–41.
[32] Romano D, Brandmeier BD, Sun YB, Trentham DR, Irving M. Orientation of the N-terminal lobe of the myosin regulatory light chain in skeletal muscle fibers. Biophys J 2012;102:1418–26.
[33] Kumar VS, O'Neall-Hennessey E, Reshetnikova L, Brown JH, Robinson H, Szent-Gyorgyi AG, et al. Crystal structure of a phosphorylated light chain domain of scallop smooth-muscle myosin. Biophys J 2011;101:2185–9.
[34] Woodhead JL, Zhao FQ, Craig R, Egelman EH, Alamo L, Padron R. Atomic model of a myosin filament in the relaxed state. Nature 2005;436:1195–9.
[35] Zoghbi ME, Woodhead JL, Moss RL, Craig R. Three-dimensional structure of vertebrate cardiac muscle myosin filaments. Proc Natl Acad Sci U S A 2008;105:2386–90.
[36] Al-Khayat HA, Kensler RW, Squire JM, Marston SB, Morris EP. Atomic model of the human cardiac muscle myosin filament. Proc Natl Acad Sci U S A 2013;110:318–23.
[37] Baumann BA, Taylor DW, Huang Z, Tama F, Fagnant PM, Trybus KM, et al. Phosphorylated smooth muscle heavy meromyosin shows an open conformation linked to activation. J Mol Biol 2012;415:274–87.
[38] Rayment I, Holden HM, Whittaker M, Yohn CB, Lorenz M, Holmes KC, et al. Structure of the actin–myosin complex and its implications for muscle contraction. Science 1993;261:58–65.
[39] Jeacocke SA, England PJ. Phosphorylation of myosin light chains in perfused rat heart. Effect of adrenaline and increased cytoplasmic calcium ions. Biochem J 1980;188:763–8.
[40] Hidalgo C, Wu Y, Peng J, Siems WF, Campbell KB, Granzier H. Effect of diastolic pressure on MLC2v phosphorylation in the rat left ventricle. Arch Biochem Biophys 2006;456:216–23.
[41] Davis JS, Hassanzadeh S, Winitsky S, Wen H, Aletras A, Epstein ND. A gradient of myosin regulatory light-chain phosphorylation across the ventricular wall supports cardiac torsion. Cold Spring Harb Symp Quant Biol 2002;67:345–52.
[42] Walker LA, Medway AM, Walker JS, Cleveland Jr JC, Buttrick PM. Tissue procurement strategies affect the protein biochemistry of human heart samples. J Muscle Res Cell Motil 2011;31:309–14.
[43] Jiang Y, Wang Y, Wang T, Hawke DH, Zheng Y, Li X, et al. PKM2 phosphorylates MLC2 and regulates cytokinesis of tumour cells. Nat Commun 2014;5:5566.
[44] Venema RC, Raynor RL, Noland Jr TA, Kuo JF. Role of protein kinase C in the phosphorylation of cardiac myosin light chain 2. Biochem J 1993;294(Pt 2):401–6.
[45] Chang AN, Chen G, Gerard RD, Kamm KE, Stull JT. Cardiac myosin is a substrate for zipper-interacting protein kinase (ZIPK). J Biol Chem 2010;285:5122–6.
[46] Kast D, Espinoza-Fonseca M, Yi C, Thomas DD. Phosphorylation-induced structural changes in smooth muscle myosin regulatory light chain. Proc Natl Acad Sci U S A 2010;107:8207–12.
[47] Hwang PM, Cai F, Pineda-Sanabria SE, Corson DC, Sykes BD. The cardiac-specific N-terminal region of troponin I positions the regulatory domain of troponin C. Proc Natl Acad Sci U S A 2014;111:14412–7.
[48] Levine RJ, Chantler PD, Kensler RW, Woodhead JL. Effects of phosphorylation by myosin light chain kinase on the structure of Limulus thick filaments. J Cell Biol 1991;113:563–72.
[49] Hooijman P, Stewart MA, Cooke R. A new state of cardiac myosin with very slow ATP turnover: a potential cardioprotective mechanism in the heart. Biophys J 2011;100:1969–76.
[50] Farman GP, Miller MS, Reedy MC, Soto-Adames FN, Vigoreaux JO, Maughan DW, et al. Phosphorylation and the N-terminal extension of the regulatory light chain help orient and align the myosin heads in *Drosophila* flight muscle. J Struct Biol 2009;168:240–9.
[51] Wang Y, Ajtai K, Burghardt TP. Ventricular myosin modifies *in vitro* step-size when phosphorylated. J Mol Cell Cardiol 2014;72:231–7.
[52] Ratti J, Rostkova E, Gautel M, Pfuhl M. Structure and interactions of myosin-binding protein C domain C0: cardiac-specific regulation of myosin at its neck? J Biol Chem 2011;286:12650–8.